Institutionen för systemteknik
Department of Electrical Engineering

Examensarbete

Linear Precoding Performance of Massive MU-MIMO Downlink System

Examensarbete utfört i Kommunikationssystem
vid Tekniska högskolan i Linköping
av

Eakkamol Pakdeejit

LiTH-ISY-EX--13/4705--SE

Linköping 2013

Linköpings universitet

TEKNISKA HÖGSKOLAN

Linear Precoding Performance of Massive MU-MIMO Downlink System

Examensarbete utfört i Kommunikationssystem
vid Tekniska högskolan i Linköping
av

Eakkamol Pakdeejit

LiTH-ISY-EX--13/4705--SE

Handledare:	**Hien Quoc Ngo**
	ISY, Linkopings universitet
Examinator:	**Dr. Daniel Persson**
	ISY, Linkopings universitet

Linköping, 31 May, 2013

Titel
Title
Svensk titel

Linear Precoding Performance of Massive MU-MIMO Downlink System

Författare   Eakkamol Pakdeejit
Author

Sammanfattning
Abstract

Nowadays, multiuser Multiple-In Multiple-Out systems (MU-MIMO) are used in a new generation wireless technologies. Due to that wireless technology improvement is ongoing, the numbers of users and applications increase rapidly. Then, wireless communications need the high data rate and link reliability at the same time. Therefore, MU-MIMO improvements have to consider 1) providing the high data rate and link reliability, 2) support all users in the same time and frequency resource, and 3) using low power consumption. In practice, the interuser interference has a strong impact when more users access to the wireless link. Complicated transmission techniques such as interference cancellation should be used to maintain a given desired quality of service. Due to these problems, MU-MIMO with very large antenna arrays (known as massive MIMO) are proposed. With a massive MU-MIMO system, we mean a hundred of antennas or more serving tens of users. The channel vectors are nearly orthogonal, and then the interuser interference is reduced significantly. Therefore, the users can be served with high data rate simultaneously. In this thesis, we focus on the performance of the massive MU-MIMO downlink where the base station uses linear precoding techniques to serve many users over Rayleigh and Nakagami-m fading channels.

Abstract

Nowadays, multiuser Multiple-In Multiple-Out systems (MU-MIMO) are used in a new generation wireless technologies. Due to that wireless technology improvement is ongoing, the numbers of users and applications increase rapidly. Then, wireless communications need the high data rate and link reliability at the same time. Therefore, MU-MIMO improvements have to consider 1) providing the high data rate and link reliability, 2) support all users in the same time and frequency resource, and 3) using low power consumption. In practice, the interuser interference has a strong impact when more users access to the wireless link. Complicated transmission techniques such as interference cancellation should be used to maintain a given desired quality of service. Due to these problems, MU-MIMO with very large antenna arrays (known as massive MIMO) are proposed. With a massive MU-MIMO system, we mean a hundred of antennas or more serving tens of users. The channel vectors are nearly orthogonal, and then the interuser interference is reduced significantly. Therefore, the users can be served with high data rate simultaneously. In this thesis, we focus on the performance of the massive MU-MIMO downlink where the base station uses linear precoding techniques to serve many users over Rayleigh and Nakagami-m fading channels.

Acknowledgments

Contents

Notation

v	Scalar a
$\boldsymbol{v}$	Vector $\boldsymbol{v}$
$\boldsymbol{V}$	Matrix $\boldsymbol{V}$
$\mathbb{R}$	Set of real numbers
$\mathbb{C}$	Set of complex numbers
$(\cdot)^*$	Complex conjugate
$(\cdot)^T$	Transpose of matrix
$tr(\cdot)$	Trace of square matrix
$(\cdot)^{-1}$	Inverse of matrix
$\boldsymbol{I}_N$	Identity matrix with size N
$\mathbb{E}[\cdot]$	Mean of the random variable
$\|\cdot\|$	Norm of vector
$|\cdot|$	Absolute value
$\mathcal{CN}(0, \sigma^2)$	Circularly symmetric complex Gaussian random variable with zero mean and variance σ^2
$\mathcal{N}(0, \sigma^2)$	Gaussian random variable with zero mean and variance σ^2

Abbreviation

MIMO	Multiple-in and multiple-out
MU-MIMO	Multiuser multiple-in and multiple-out
LTE	Long Term Evolution
OFDM	Orthogonal frequency division multiplexing
i.i.d.	Independent and identically distributed
MMSE	Minimum mean square error
ZF	Zero forcing
MRT	Maximum ratio transmission
SDMA	Space division multiple access
CSI	Channel state information
MSE	Mean square error
PDF	Probability density function
SNR	Signal to noise ratio
SINR	Signal to interference plus noise ratio

List of Figures

Chapter 1

Introduction

1.1 Background

Multiple-In Multiple-Out (MIMO) technology is now being introduced in modern wireless broadband standards e.g., Long Term Evolution Advanced (LTE-Advanced). According to 3GPP LTE standard, LTE permits for up to 8 antennas at the base station [1]. The goal of wireless communication improvement is to provide a high data rate for each user. At present, the latest wireless technology uses MU-MIMO system for that reason. Theoretically, increasing the number of antennas at the transmitter or receiver can improve the performance of the system in terms of data throughput and link reliability. Besides improving the data throughput and link reliability, MU-MIMO enables to save the transmitter energy, owing to the array gain [2]. On a channel that fluctuates rapidly as a ten of time and frequency, and where the situation allows coding across many channel coherence intervals, the achievable rate scales as $\min(M, K) \log(1 + \texttt{SNR})$ [1] where M is the number of antennas, and K is the number of users. In multiuser systems, the benefits are more attractive because such systems offer the possibility to transmit simultaneously to several users [1].

With a multiuser MIMO (MU-MIMO) system, the base station is equipped with multiple antennas and serves several users. Commonly, the base station communicates with many users through orthogonal channels. More precisely, the base station communicates with each user in a separate time and frequency resource [2]. However, the higher data rate can be achieved if the base station communicates with the user in the same time-frequency resources. The main challenge of this system is interuser interference, which significantly reduces the system performance. In the downlink, dirty-paper coding can be used to reduce the effect of interuser interference [3], [4]. However, it induces a significant complexity for the implementation.

Recently, massive MU-MIMO (as know as very large MU-MIMO) system has attracted a lot of interest. massive MU-MIMO refers to MU-MIMO where the base station equipped very large antenna arrays serves tens of single-antenna users simultaneously. Very large means hundreds of antennas. When the number of an-

tennas increases, the random channel vectors between the users and base station become nearly orthogonal [1]. Other important advantage of massive MU-MIMO systems is that they enable us to reduce the transmitted power. On the uplink, reducing the power of the terminals will save their battery life. On the downlink, much of the electrical base station power is spent by power amplifiers and associated circuits and cooling systems [5]. Hence reducing the RF power would help in cutting the electricity of the base station.

Massive MU-MIMO technology is now attracting substantial attention from both academia and industry [1–17]. This motivates us to work on this topic. Most of the studies considered the uplink performance. Here, we study massive MU-MIMO downlink system with linear precoding techniques. We consider the system performance when the number of antennas and the number of users are large. We study the system performance in terms of data throughput and energy for different propagation environments.

In addition to study the massive MU-MIMO system performance, we are interested in the performance comparisons among linear precoders: Minimum Mean Square Error (MMSE), Zero Forcing (ZF), and Maximum Ratio Transmission (MRT) precoding. Hypothetically, the precoding is known as Space Division Multiple Access. Each linear precoding shows the best performance with each signal power regime. For the comparison between MRT and ZF, MRT gives better performance at low signal to noise ratio (SNR) while ZF performs better at high SNR. MMSE gives the best performance across the entire SNR. These properties are used for improving the performance of massive MU-MIMO in different propagation environments.

1.2 Problem Description

To study the performance of the massive MU-MIMO downlink system. Generally, increasing the number of antennas at the base station gains the achievable rate for each user in its cell [2]. In addition to gain the achievable rate, it gains the energy efficiency in terms of radiation from the base station. However, the different propagation environments give the different system performances. Consequently, we consider the effect of massive MU-MIMO system where the base station is equipped with a large number of antennas and serves tens of single-antenna users Nevertheless, the number of users is not greater than the number of antennas.

To analyze massive MU-MIMO downlink system, we investigate the performance of linear precoding. Linear precoding is a simple processing where the transmitted signal vector is obtained by multiplying the information data vector with a linear precoding matrix. Conventionally, in single-user systems, each user maximizes the data throughput for itself, but in case of MU-MIMO system, the transmitter cannot transmit all users with maximum data throughput simultaneously. It needs more processing to transmit the appropriate data. There always exists a trade off between the system performance and implementation complexity. Linear precoding is simple and hence, it has low deployment cost. We consider the linear precoding techniques at the base station and study the performance of each

linear precoding with different propagation environments, and different SNR.

1.3 Goals of Thesis

The goals of this thesis are to analyze the effects in a massive MU-MIMO downlink system with linear precoding and different channel models. Firstly, we derive the optimal linear precoding. Moreover, we simulate the channel models with computer software. We calculate the spectral efficiency and the energy efficiency to analyze the effect of massive MU-MIMO downlink system over different channel models.

Chapter 2

MU-MIMO system

This chapter will describe the principle of MU-MIMO downlink system, which includes channel estimation, linear precoding techniques, Rayleigh fading channel, Nakagami-m fading channel. Further, we introduce basic theories.

2.1 The Principle of MU-MIMO

A MU-MIMO system refers to the system where the base station communicates with several users simultaneously. The base station and the user can be equipped with multiple antennas. The MU-MIMO system enables many parallel communications in the same time and frequency resource that called Space Division Multiple Access (SDMA). MU-MIMO system has many advantages: [18]

 • *increased data rate*, due to that base station is equipped with many antennas, and hence, it sends the independent data streams to many users simultaneously. This is called multiplexing gain.

 • *link reliability*, due to that antennas generate a lot of communication paths that the radio signal can propagate over. This is called diversity gain.

 • *improving the energy efficiency*, due to that base station is able to focus its transmission power into the spatial direction where each user is located This is called array gain.

By these advantages, MU-MIMO technology is used in the wireless communication standards. More base station antennas can be equipped with; better performance can be achieved. The current LTE allows up to 8 antennas at the base station.

2.2 MU-MIMO Downlink System

Consider a MU-MIMO downlink system, which includes one base station equipped with M antennas, and K single-antenna users. See Figure 2.1. We assume that K users share the same time-frequency resources. We are interested in the system where $M \gg K$. This system refers to a massive MU-MIMO. We further assume

9
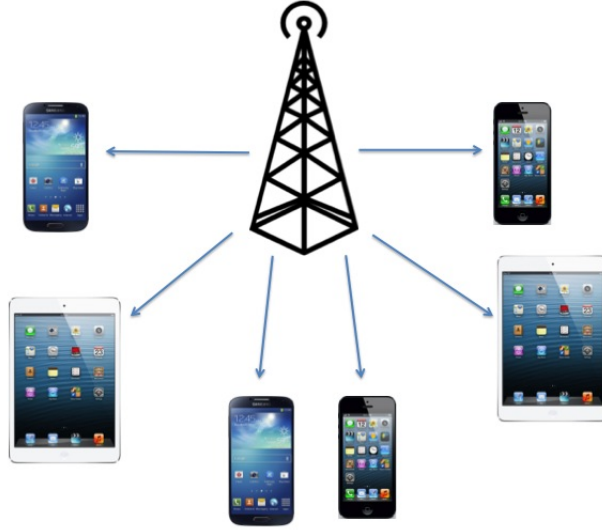
Figure 2.1. Multiuser MIMO downlink system

that the channels will stay constant during a coherence interval of T symbols. The downlink transmission will occur in two phases: training phase and downlink data transmission phase. See Figure 2.2, where τ is the coherence duration used for the training phase. In the training phase, the base station estimates the channel state information (CSI) from K users based on the received pilot sequences in the uplink. The base station uses this CSI and linear precoding schemes to process the transmit data. More details of the channel estimation scheme and downlink data transmission will be discussed next section.

2.3   Channel Estimation

Typically, the channel estimation is done on the downlink. More precisely, each user estimates the channel using pilot sequences transmitted from the base station, and then it feedbacks this CSI to the base station. This channel estimation over-head will be proportional to the number of base station antennas. Therefore, with massive MU-MIMO system, this is very inefficient. Thus, here we assume that the channel is estimated at the base station via uplink pilots, assuming channel reciprocity.

Let τ in duration used for channel estimation. Each user is assigned an orthogonal pilot sequence of τ symbols where $\tau \geq K$. The $M \times \tau$ received pilot matrix at the base station is given by [19]

$$\boldsymbol{Y}_p = \sqrt{p_p}\boldsymbol{H}\boldsymbol{\Phi}^T + \boldsymbol{N}_p \tag{2.1}$$

Figure 2.2. Downlink transmission protocol

where $\boldsymbol{\Phi} \in \tau \times K$ is the pilot sequence used by K users satisfying $\boldsymbol{\Phi}^H \boldsymbol{\Phi} = \boldsymbol{I}_K$; $\boldsymbol{N}_p \in \mathbb{C}^{M \times \tau}$ is the additive noise at the base station; $\boldsymbol{H}$ is an $M \times K$ channel matrix between the K users and the base station; and $p_p = \tau p_u$, where p_u is the transmitted power of each user. From (2.1), The channel can be estimated from [19]:

$$\tilde{\boldsymbol{Y}}_p = \sqrt{p_p} \boldsymbol{H} + \boldsymbol{W} \tag{2.2}$$

where $\tilde{\boldsymbol{Y}}_p = \boldsymbol{Y}_p \boldsymbol{\Phi}^*$ and $\boldsymbol{W} = \boldsymbol{N}_p \boldsymbol{\Phi}^*$

Let $\boldsymbol{y}_k$ and $\boldsymbol{w}_k$ be the kth columns of $\tilde{\boldsymbol{Y}}_p$ and $\boldsymbol{W}$ respectively. Then [19],

$$\tilde{\boldsymbol{y}}_{p,k} = \sqrt{p_p} \boldsymbol{h}_k + \boldsymbol{w}_k \tag{2.3}$$

Assuming that the base station uses MMSE channel estimation, the channel estimate of $\boldsymbol{h}_k$ is given by [19]

$$\tilde{\boldsymbol{h}}_k = \arg \min_{\tilde{\boldsymbol{h}}_k \in \mathbb{C}^M} \mathbb{E}_{\boldsymbol{h}_k, \tilde{\boldsymbol{y}}_{p,k}} \left[\left\| \tilde{\boldsymbol{h}}_k - \boldsymbol{h}_k \right\|^2 \right] \tag{2.4}$$

Finally, we obtain the channel estimate of $\boldsymbol{h}_k$ as [19]

$$\begin{aligned} \tilde{\boldsymbol{h}}_k &= \frac{\sqrt{p_p}}{p_p + 1} \tilde{\boldsymbol{y}}_{p,k} \\ &= \frac{p_p}{p_p + 1} \boldsymbol{h}_k + \frac{\sqrt{p_p}}{p_p + 1} \boldsymbol{w}_k \end{aligned} \tag{2.5}$$

With large p_p or τ, we obtain a perfect channel estimate. This is the case that we consider in this thesis.

2.4 Downlink Data Transmission

The base station uses the channel estimates obtained from channel estimation phase to process the signals before transmitting them to K users. We assume
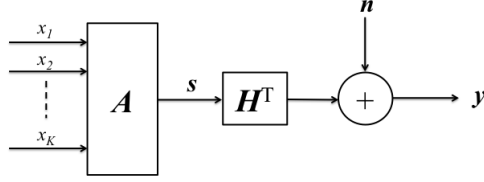
Figure 2.3. The system model

that the base station uses linear precoding techniques. Furthermore, we assume that the base station has perfect CSI. This assumption is reasonable under the scenarios that the training power is large or the coherent interval is large (and hence, we can spend large τ for training). See (2.5).

Let $\boldsymbol{A} \in \mathbb{C}^{M \times K}$ be a linear precoding matrix, and $\boldsymbol{x}$ is a $K \times 1$ information vector, where x_k is data symbol for user k, where $\mathbb{E}\left[|x_k|^2\right] = 1$. The transmitted vector $\boldsymbol{s}$ can be written as $\boldsymbol{s} = \boldsymbol{A}\boldsymbol{x}$, and its average transmission power is constrained by $\mathbb{E}\left[\|\boldsymbol{s}\|^2\right] = \text{tr}\left(\boldsymbol{A}^H\boldsymbol{A}\right) = P_{tr}$. Then, the received vector at the K users is given by

$$y = \boldsymbol{H}^T\boldsymbol{s} + \boldsymbol{n} \tag{2.6}$$

where $\boldsymbol{n}$ is a $K \times 1$ additive noise vector, where $n_k \in \mathcal{CN}(0, 1)$. We use this model to find the linear precoding matrix in order to study the performance of massive MU-MIMO system. The system model is shown in Figure 2.3.

2.5   The Linear Precoding

We consider the linear precoding techniques, which include MMSE, ZF, and MRT.

2.5.1   MMSE Precoding

MMSE precoding is the optimal linear precoding in MU-MIMO downlink system. This technique is generated by the mean square error (MSE) method. Owing to average power at each transmitted antenna is constrained, Lagrangian optimization method is used for obtaining this precoder.

Firstly, we start to consider the MSE of the signal. The MSE can be written as [20]

$$\epsilon = \mathbb{E}\left[\|\beta\boldsymbol{y} - \boldsymbol{x}\|^2\right] \tag{2.7}$$

where β is a scalar of Wiener filter.

Firstly, we find $\boldsymbol{A}$ and β to minimize the MSE under the power constraint. Then,

$$\left[\hat{\boldsymbol{A}}, \hat{\beta}\right] = \arg\min_{\boldsymbol{A}, \beta} \epsilon$$
$$\text{s.t.}\,\mathbb{E}\left[\|\boldsymbol{s}\|^2\right] = P_{tr} \tag{2.8}$$

To solve the optimization problem, the Lagrangian method is used for this problem. Then,

$$\mathcal{L}\left(\boldsymbol{A}, \beta, \lambda\right) = \mathbb{E}\left[\|\beta\boldsymbol{y} - \boldsymbol{x}\|^2\right] - \lambda tr\left(\boldsymbol{s}^H\boldsymbol{s} - P_{tr}\right) \tag{2.9}$$

where $\lambda \in \mathbb{R}$ is the Lagrangian factor. In order to find $\boldsymbol{A}$, β, and λ to minimize the MSE, we take derivatives with respect to $\boldsymbol{A}$, and λ. As a result, $\boldsymbol{A}_{\text{MMSE}}$ can be expressed as

$$\boldsymbol{A}_{\text{MMSE}} = \frac{1}{\beta}\boldsymbol{H}^*\left(\boldsymbol{H}^T\boldsymbol{H}^* + \frac{K}{P_{tr}}\boldsymbol{I}_K\right)^{-1} \tag{2.10}$$

where

$$\beta = \sqrt{\frac{\text{tr}(\boldsymbol{B}\boldsymbol{B}^H)}{P_{tr}}} \tag{2.11}$$

where $\boldsymbol{B} = \boldsymbol{H}^*\left(\boldsymbol{H}^T\boldsymbol{H}^* + \frac{K}{P_{tr}}\boldsymbol{I}_K\right)^{-1}$.

The detail derivations of (2.10) and (2.11) are shown in Appendix.

2.5.2 ZF Precoding

ZF precoding is one technique of linear precoding in which the interuser interference can be cancelled out at each user. This precoding is assumed to implement a pseudo-inverse of the channel matrix.

ZF approaches MMSE when $P_{tr} \to \infty$. Therefore, from (2.10), $\boldsymbol{A}_{\text{ZF}}$ can be expressed as

$$\boldsymbol{A}_{\text{ZF}} = \frac{1}{\beta}\boldsymbol{H}^*\left(\boldsymbol{H}^T\boldsymbol{H}^*\right)^{-1} \tag{2.12}$$

where

$$\beta = \sqrt{\frac{\text{tr}(\boldsymbol{B}\boldsymbol{B}^H)}{P_{tr}}} \tag{2.13}$$

where $\boldsymbol{B} = \boldsymbol{H}^*\left(\boldsymbol{H}^T\boldsymbol{H}^*\right)^{-1}$.

2.5.3 MRT Precoding

One of the common methods is MRT which maximizes the SNR. MRT works well in the MU-MIMO system where the base station radiates low signal power to the users.

MRT approaches MMSE when $P_{tr} \rightarrow 0$. Hence, from (2.10), $\boldsymbol{A}_{\mathrm{MRT}}$ can be expressed as

$$\boldsymbol{A}_{\mathrm{MRT}} = \frac{1}{\beta}\boldsymbol{H}^* \tag{2.14}$$

where

$$\beta = \sqrt{\frac{\mathrm{tr}(\boldsymbol{B}\boldsymbol{B}^H)}{P_{tr}}} \tag{2.15}$$

where $\boldsymbol{B} = \boldsymbol{H}^*$.

2.6 Rayleigh Fading Channel

In the wireless communication, it is difficult to find the exact channel properties because of multipath propagation in each environment. Nonetheless, channel models are used for analyzing system performance. One of the channel models, which is used for modeling the channel fading, is a Rayleigh fading channel.

The model assumption is that the summation of many statistically independent reflected and scattered paths with random amplitudes is an independent and identically distributed (i.i.d) complex Gaussian random variable. The element of the channel matrix can be written in a complex number form as [21]

$$h_{ij} = c + jd$$

The joint probability density function (PDF) can be written as

$$f_{c,d}(c,d) = \frac{1}{2\pi\sigma^2} \exp\left(-\frac{c^2 + d^2}{2\sigma^2}\right)$$

Expressing h_{ij} in polar form we obtain

$$h_{ij} = r\exp(j\theta)$$

where

$$r = \sqrt{c^2 + d^2}$$

$$\theta = \arctan\frac{d}{c}$$

From polar form, we can write the joint PDF of R and θ by

$$f_{R,\theta}(r,\theta) = \frac{r}{2\pi\sigma^2} \exp\left(-\frac{r^2}{2\sigma^2}\right)$$

By integration with θ we obtain the PDF of R as

$$p_R(r) = \frac{r}{\sigma^2} \exp\left(-\frac{r^2}{2\sigma^2}\right)$$

The PDF of R is same as Rayleigh distributed. By above properties, Rayleigh fading channel can be described in terms of amplitude and phase.

The channel coefficient of complex Rayleigh fading is generated by two Gaussian random variables where each variable has zero mean and variance 0.5. Each Gaussian random variable is put in the real part and imaginary part. Then, the channel coefficient of Rayleigh fading channel is given by

$$h_{\text{Rayleigh}} = c + jd$$

where $c \in \mathcal{N}\left(0, \frac{1}{\sqrt{2}}\right)$ and $d \in \mathcal{N}\left(0, \frac{1}{\sqrt{2}}\right)$.

2.7 Nakagami-m Fading Channel

A Nakagami-m fading has been widely used to model the fading distribution in various wireless channels. Then, Nakagami-m fading channel is used for modeling the channel.

Typically Nakagami-m fading can be described by the Nakagami-m distribution. The PDF of Nakagami-m fading channel can be expressed as [22]

$$p_R(R) = \frac{2m^m R^{2m-1}}{\Omega^m \Gamma(m)} \exp\left(-\frac{mR^2}{\Omega}\right)$$

where the amplitude of channel $R \geq 0$, $\Omega = E(R^2)$ is an average fading power with $m \geq \frac{1}{2}$, and $\Gamma(m)$ is the gamma function. m and Ω can be expressed as

$$m = \frac{E^2[R^2]}{Var[R]}$$

$$\Omega = E[R^2]$$

The PDF gets its characteristics from the m value. The parameter m is a shape factor of the Nakagami-m distribution, which describes fading degree of the propagation. For $m = 1$, The Nakagami-m distribution has the same properties as the Rayleigh distribution. That means Nakagami-m fading channel with $m = 1$ acts as a Rayleigh fading channel. For, $m > 1$, the fluctuation of signal amplitude reduces comparing with Rayleigh fading. When $m \to \infty$, Nakagami-m fading becomes non-fading. For $m = 0$, Nakagami-m fading acts as a Ricean fading channel.

The complex Nakagami-m coefficient is generated by m-Gaussian random variables where each random value has zero mean and variance $\frac{1}{2m}$ in both the real and imaginary parts $X \sim \mathcal{N}\left(0, \frac{1}{\sqrt{2m}}\right)$, $Y \sim \mathcal{N}\left(0, \frac{1}{\sqrt{2m}}\right)$ [22]. In the real part, All

Gaussian random variables are squared and summed. The result gives a Chi-square distributed random number. This number is given by

$$Z_{Re}^2 = X_1^2 + X_2^2 + ... + X_m^2$$

This same process is used for the imaginary part. Finally, we obtain the amplitude of the Nakagami-m distribution. For the phase of Nakagami-m fading channel, the phase is randomized by the uniform distribution with interval $[0, 2\pi]$. Therefore, the complex coefficient of the Nakagami-m fading channel can be written in polar form as [22]

$$h_{\text{Nakagami-}m} = G \exp(j\theta)$$

where $G = \sqrt{Z_{\text{Re}}^2 + Z_{\text{Im}}^2}$, and θ is unif$(0, 2\pi)$.

Chapter 3

Performance Analysis

This chapter will describe the performance analysis, which includes the achievable rate, the energy efficiency, and implementation.

3.1   The Achievable Rate

The system performance can be defined by several methods. One of method, to quantify the system performance, is the achievable rate. The achievable rate is followed by Shannon theorem. This theory tells the maximum rate, which the transmitter can transmit over the channel. This section will describe the achievable rate, and assumes that the channel is ergodic and that all parameters are Gaussian random processes.

From (2.6), let y_k and x_k be the kth elements of the $K \times 1$ vectors $\boldsymbol{y}$ and $\boldsymbol{x}$ respectively. Then, the y_k can be expressed as

$$y_k = \boldsymbol{h}_k^T \boldsymbol{a}_k x_k + \sum_{i=1,i\neq k}^{K} \boldsymbol{h}_k^T \boldsymbol{a}_i x_i + n_k \tag{3.1}$$

The energy of desired signal is given by

$$\mathbb{E}\left[\left|\boldsymbol{h}_k^T \boldsymbol{a}_k x_k\right|^2\right] = |\boldsymbol{h}_k^T \boldsymbol{a}_k|^2 \mathbb{E}[|x_k|^2]$$
$$= |\boldsymbol{h}_k^T \boldsymbol{a}_k|^2 \tag{3.2}$$

The interuser interference plus noise energy is given by

$$\mathbb{E}\left[\left|\sum_{i=1,i\neq k}^{K} \boldsymbol{h}_k^T \boldsymbol{a}_i x_i + n_k\right|^2\right] = \sum_{i=1,i\neq k}^{K} |\boldsymbol{h}_k \boldsymbol{a}_i|^2 \, \mathbb{E}\left[|x_i|^2\right] + \mathbb{E}\left[|n_k|^2\right]$$
$$= \sum_{i=1,i\neq k}^{K} |\boldsymbol{h}_k \boldsymbol{a}_i|^2 + 1 \tag{3.3}$$

From Shannon theorem, the channel capacity over Additive White Gaussian Noise channel is derived by [23]

$$R = \log_2(1 + \texttt{SNR}) \quad (bits/s/Hz)$$

With MU-MIMO downlink system, the transmitter must know channel state information. CSI is a key of multiuser communication. Typically, the transmitter transmits multiple data streams to each user simultaneously and selectively with CSI [24]. According to section 2.3, all receivers send channel estimation feedback to the transmitter on the reverse link, so the transmitter obtains CSI. Hence, the transmitter communicates all receivers with perfect CSI. With a MU-MIMO system, the interference consists of additive noise and interference between the users themselves. Then, the achievable rate of kth user for MU-MIMO downlink system can be expressed as

$$R_k = \mathbb{E}\left[\log_2\left(1 + \texttt{SINR}_k\right)\right] \quad (bits/s/Hz) \tag{3.4}$$

From (3.2) and (3.3), (3.4) can be written as

$$R_k = \mathbb{E}\left[\log_2\left(1 + \frac{|\boldsymbol{h}_k^T \boldsymbol{a}_k|^2}{1 + \sum_{i=1, i\neq k}^K |\boldsymbol{h}_k \boldsymbol{a}_i|^2}\right)\right] \tag{3.5}$$

3.1.1   The Achievable Rate with MMSE Precoding

From (2.10), we obtain the received vector with MMSE as

$$\boldsymbol{y} = \frac{1}{\beta}\boldsymbol{H}^T\left[\boldsymbol{H}^*\left(\boldsymbol{H}^T\boldsymbol{H}^* + \frac{K}{P_{tr}}\boldsymbol{I}_K\right)^{-1}\right]\boldsymbol{x} + \boldsymbol{n} \tag{3.6}$$

where $\beta = \sqrt{\frac{\text{tr}\left(\boldsymbol{H}^T\boldsymbol{H}^*\left(\boldsymbol{H}^T\boldsymbol{H}^* + \frac{K}{P_{tr}}\boldsymbol{I}_K\right)^{-2}\right)}{P_{tr}}}$

Let y_k, x_k, and n_k be the kth elements of $K \times 1$ vectors $\boldsymbol{y}$, $\boldsymbol{x}$, and $\boldsymbol{n}$ respectively and we define the kth column of $\boldsymbol{A}_{\text{MMSE}}$ as

$$\boldsymbol{a}_k = \boldsymbol{H}^*\boldsymbol{\Lambda}_k \tag{3.7}$$

where $\boldsymbol{\Lambda}_k$ is the kth column of $\left(\boldsymbol{H}^T\boldsymbol{H}^* + \frac{K}{P_{tr}}\boldsymbol{I}_K\right)^{-1}$. From (3.7), the received vector of kth user with MMSE is given by

$$y_k = \frac{1}{\beta}\boldsymbol{h}_k^T\boldsymbol{H}^*\boldsymbol{\Lambda}_k x_k + \frac{1}{\beta}\sum_{i=1, i\neq k}^K \boldsymbol{h}_k^T\boldsymbol{H}^*\boldsymbol{\Lambda}_i x_i + n_k \tag{3.8}$$

The achievable rate of kth user with MMSE is given by

$$R_k^{\text{MMSE}} = \mathbb{E}\left[\log_2\left(1 + \frac{\frac{1}{\beta^2}|\boldsymbol{h}_k\boldsymbol{H}^*\boldsymbol{\Lambda}_k|^2}{1 + \frac{1}{\beta^2}\sum_{i=1, i\neq k}^K \left|\boldsymbol{h}_k^T\boldsymbol{H}^*\boldsymbol{\Lambda}_i\right|^2}\right)\right] \tag{3.9}$$

3.1.2   The Achievable Rate with ZF precoding

From (2.12), we obtain the received vector with ZF as

$$y = \frac{1}{\beta} \boldsymbol{H}^T \left[\boldsymbol{H}^* \left(\boldsymbol{H}^T \boldsymbol{H}^* \right)^{-1} \right] \boldsymbol{x} + \boldsymbol{n} \tag{3.10}$$

where $\beta = \sqrt{\frac{\operatorname{tr}(\boldsymbol{H}^T \boldsymbol{H}^* (\boldsymbol{H}^T \boldsymbol{H}^*)^{-2})}{P_{tr}}}$

Let y_k, x_k, and n_k be the kth elements of $K \times 1$ vectors $\boldsymbol{y}$, $\boldsymbol{x}$, and $\boldsymbol{n}$ respectively and we define the kth column of $\boldsymbol{A}_{\mathrm{ZF}}$ as

$$\boldsymbol{a}_k = \boldsymbol{H}^* \boldsymbol{g}_k \tag{3.11}$$

where $\boldsymbol{g}_k$ is the kth column of $(\boldsymbol{H}^T \boldsymbol{H}^*)^{-1}$. From (3.11), the received vector of kth user with ZF is given by

$$y_k = \frac{1}{\beta} \boldsymbol{h}_k^T \boldsymbol{H}^* \boldsymbol{g}_k x_k + \frac{1}{\beta} \sum_{i=1, i \neq k}^{K} \boldsymbol{h}_k \boldsymbol{H}^* \boldsymbol{g}_i x_i + n_k \tag{3.12}$$

The achievable rate of kth user with ZF is given by

$$R_k^{\mathrm{ZF}} = \mathbb{E} \left[\log_2 \left(1 + \frac{\frac{1}{\beta^2} \left| \boldsymbol{h}_k^T \boldsymbol{H}^* \boldsymbol{g}_k \right|^2}{1 + \frac{1}{\beta^2} \sum_{i=1, i \neq k}^{K} \left| \boldsymbol{h}_k^T \boldsymbol{H}^* \boldsymbol{g}_i \right|^2} \right) \right] \tag{3.13}$$

3.1.3   The Achievable Rate with MRT precoding

From (2.14), we obtain the received vector with MRT as

$$y = \frac{1}{\beta} \boldsymbol{H}^T \boldsymbol{H}^* \boldsymbol{x} + \boldsymbol{n} \tag{3.14}$$

where $\beta = \sqrt{\frac{\operatorname{tr}(\boldsymbol{H}^T \boldsymbol{H}^*)}{P_{tr}}}$

Let y_k, x_k, and n_k be the kth elements of $K \times 1$ vectors $\boldsymbol{y}$, $\boldsymbol{x}$, and $\boldsymbol{n}$ respectively and we define the kth column of $\boldsymbol{A}_{\mathrm{MRT}}$ as

$$\boldsymbol{a}_k = \boldsymbol{h}_k^* \tag{3.15}$$

From (3.15), the received vector of kth user with MRT is given by

$$y_k = \frac{1}{\beta} \boldsymbol{h}_k^T \boldsymbol{h}_k^* x_k + \frac{1}{\beta} \sum_{i=1, i \neq k}^{K} \boldsymbol{h}_k^T \boldsymbol{h}_i^* x_k + n_k \tag{3.16}$$

The achievable rate of kth user with MRT is given by

$$R_k^{\mathrm{MRT}} = \mathbb{E} \left[\log_2 \left(1 + \frac{\frac{1}{\beta^2} \| \boldsymbol{h}_k \|^4}{1 + \frac{1}{\beta^2} \sum_{i=1, i \neq k}^{K} \left| \boldsymbol{h}_k^T \boldsymbol{h}_i^* \right|^2} \right) \right] \tag{3.17}$$

3.2 The Energy Efficiency

The energy efficiency of a system is defined as the sum-rate (the spectral efficiency) divided by the transmit power. Generally, increasing transmit power increases the sum-rate. On the contrary, it decreases the energy efficiency.

With a single call massive MU-MIMO system with perfect CSI, the spectral efficiency is defined as

$$R_P = \sum_{k=1}^{K} R_k \tag{3.18}$$

where R_P is the spectral efficiency in bits/s/Hz and R_k is the achievable rate of user k.

The energy efficiency can be written as

$$\eta = \frac{R_P}{P_{tr}} \quad (bits/J/Hz) \tag{3.19}$$

where P_{tr} is the average transmission power at the base station (J/s).

We study the tradeoff between the energy efficiency and the spectral efficiency of massive MU-MIMO downlink system with linear precoding. We investigate the system performance with different number of antennas M and number of users K.

3.3 Implementation

We use MATLAB-2013a to generate all scenarios. Each simulation should use 10,000 channel realization to realize that the results are correct and smooth.

3.3.1 Calculating Signal to Noise Ratio

SNR is defined by the ratio between the desired signal power and noise power.

With our models, we assume that the desired signal vector $\boldsymbol{x}$ and the noise vector $\boldsymbol{n}$ are i.i.d. complex Gaussian random variables with zero mean and unit variance. Further, the transmission power is constrained. Then, the SNR is given by

$$\begin{aligned} \frac{S}{N} &= P_{tr} \\ &= 10 \log P_{tr} \quad dB \end{aligned} \tag{3.20}$$

3.3.2 Calculating Achievable Rate

At the beginning, the MU-MIMO system performance is measured by the achievable rate. We analyze the achievable rate of the user 1 because all of the users have the same achievable rate properties. Then, we measure the achievable rate only for the user 1 by measure the achievable rate of user 1 within 10,000 channel realization. After we obtain these achievable rates, we average them. The average value is used to study massive MU-MIMO downlink system performance.

3.3.3 Calculating Spectral Efficiency

After we calculate the achievable rate of user 1, we calculate the spectral efficiency by multiplication between the achievable rate of user 1 and the number of users in the system [1]. The spectral efficiency is given by (3.21). We keep this parameter to study the performance of massive MU-MIMO downlink system.

$$R_P = K \times R_k \qquad (bits/s/Hz) \qquad (3.21)$$

3.3.4 Calculating Energy Efficiency

Besides we analyze the achievable rate and the spectral efficiency, we study the performance of MU-MIMO on the downlink in term of the energy efficiency. We use (3.19) to calculate the energy efficiency. After we obtain the spectral efficiency, this parameter is divided by SNR. We obtain the energy efficiency. This parameter is brought to analyze the system performance over Rayleigh fading channel only.

Chapter 4

Simulation Results

This chapter will present the simulation results, and the practical massive MU-MIMO system.

4.1 The Massive MU-MIMO Downlink System over Rayleigh Fading Channel

We consider only single cell massive MU-MIMO system, which means no intra-cell interference. We generate the 1st and 2nd scenarios, which consist of 1) increasing the number of antenna arrays with fixing the number of users and 2) increasing the number of users, over Rayleigh fading channel. However, the limitation of models are that the number of users K is not greater than the number of antennas M. All results are shown in terms of the achievable rate versus transmission power, the spectral efficiency versus the number of antenna arrays, the spectral efficiency versus the number of users, and the energy efficiency versus the spectral efficiency.

4.1.1 Scenario 1

We start to investigate the performance of massive MU-MIMO downlink system over Rayleigh fading channel by considering the achievable rate. We choose the number of users $K = 10$. We change the number of antennas from 20 to 100. We set up the BS power from -20 to 20 dB. All results are shown in figures below.

Figure 4.1 shows the achievable rate of user 1 across the entire SNR range. This system consists of the number of antennas $M = 20$ and the number of users $K = 10$. The results show that MRT gives the better performance at low SNR. On the other sides, ZF gives better performance at high SNR. MMSE performs the best achievable rate across SNR range

Figure 4.2 shows the achievable rate of user 1 when we increase the number of antennas from 20 to 40. All results show that the system performance is improved. The achievable rates of MMSE, ZF, and MRT are increased by increasing the number of antennas. Corresponding to the results in Figure 4.1, MMSE gives the

highest achievable rate to user 1. For comparison between ZF and MRT, ZF still gives the better performance at high SNR while MRT performs the higher rate at low SNR. We observe that a point, where ZF performance is better than MRT, is moved from 0 to -5 dB SNR. Increasing the number of antennas makes ZF able to be used at low SNR.

Figure 4.3 shows the spectral efficiency versus the number of antennas at 10 dB SNR. Corresponding to the results in Figures 4.1 and 4.2, Figure 4.3 shows that all spectral efficiencies with linear precoding increased significantly by increasing the number of antennas. For example, the spectral efficiency with ZF increases from $M = 20$ to $M = 40$ around 10 bits/s/Hz.

In Figure 4.4, we study the performance of massive MU-MIMO downlink system with linear precoding in terms of energy efficiency versus the spectral efficiency. We consider $M = 20$, and 40. When we increase the spectral efficiency, the energy efficiency is decreased. The results show that MMSE gives the best energy efficiency across the entire spectral efficiency range. At high energy efficiency and low spectral efficiency, MRT gives the better performance while ZF gives the better performance at low energy efficiency and high spectral efficiency.

The results show that increasing the number of antennas gains the energy efficiency significantly. For example, at spectral efficiency 10 bits/s/Hz, the energy efficiency of the base station antennas $M = 20$ with MRT is 10 bits/J. When $M = 40$, the energy efficiency increases from 10 to 30 bits/J.

4.1.2 Scenario 2

In Scenario 1, we increase the number of base station antennas and fix the number of users. In Scenario 2, we fix the number of antennas M and increase the number of users K, which $K < M$. In this scenario, we consider $M = 40$ and $K = 10$, 15, 20, 25, 30, and 35 respectively. We choose SNR from -20 to 20 dB. All results are shown in figures below.

Figure 4.6 shows that the achievable rate of user 1 with $M = 40$ serving $K = 15$. From the comparison between Figure 4.5 and 4.6, massive MU-MIMO downlink system performance decreases significantly due to interuser interference. All achievable rates of user 1 with linear precoding are reduced around 0.5 bits/s/Hz at 20 dB SNR.

Although increasing the number of users reduces the achievable rate of user 1, MMSE gives the highest data rate. At low SNR, MRT performs the higher rate while ZF give the better performance in term of the achievable rate at the high SNR. Notice that the gap between MMSE and ZF is extended. Moreover, the SNR range where the achievable rate of user 1 with MRT is greater than one with ZF, is extended further.

In Figure 4.7, the results show the spectral efficiency versus the number of users at 10 dB SNR. The spectral efficiency with MMSE increases rapidly until $K = 25$. When $K > 25$, increasing the spectral efficiency is very slow. After $K > 30$, the spectral efficiency is decreased slightly. As the result, $K = 30$ is an optimal number with MMSE.

According to MMSE result, the spectral efficiency with ZF increases quickly

by increasing the users. Until $K > 25$, the spectral efficiency is dropped rapidly. With ZF, the optimal number of users is around 25 for a massive MU-MIMO downlink system over Rayleigh fading channel with $M = 40$.

On the other hand, the spectral efficiency versus the number of users with MRT increases slowly although the number of users K increases. However, the spectral efficiency with MRT is less than MMSE and ZF.

Figure 4.8 shows the energy efficiency versus the spectral efficiency with linear precoding at the number of users. The results show that with MMSE and MRT, the energy efficiencies increase by increasing the number of users K. For example, with $K = 15$ and 25, the energy efficiencies with MRT are 0.3 and 8 bits/J at spectral efficiency 30 bits/s/Hz. On the contrary, at 30 bits/s/Hz spectral efficiency, the energy efficiencies with ZF are around 18 and 15 bits/s/Hz. Moreover, MMSE is the best in term of the energy efficiency. At low spectral efficiency and high energy efficiency, MRT is better while ZF is better at high energy efficiency and low spectral efficiency.

4.2 The Massive MU-MIMO Downlink System over Nakagami-m Fading Channel

Over Nakagami-m fading channel, we simulate two scenarios to study the system performance. Firstly, we investigate the system performance when we change the parameter m. Furthermore, we study the performance when we increase the number of antennas M at the low SNR. In Scenario 4, we increase the number of users K and change the parameter m at the low SNR. In Scenario 3, all results are shown in terms of the spectral efficiency versus the number of antennas M. In Scenario 4, all results are shown in terms of the spectral efficiency versus the number of users K.

4.2.1 Scenario 3

In Scenario 3, we change the number of antennas M with different parameters m. We choose the number of users $K = 2$. We change the number of antennas from 2 to 20. Furthermore, we choose SNR at 0 dB. All results are shown in figures below.

The results show that increasing the parameter m improves the system performance in term of the spectral efficiency. Over Nakagami-m fading channel, the spectral efficiency with linear precoding increases significantly. For instance, with $m = 2$, the achievable rate of user 1 with MMSE is the better performance than $m = 1$. When the parameter m is large, the spectral efficiency with MMSE increases significantly.

Figures 4.9, 4.10, and 4.11 show the spectral efficiency versus the number of antennas with different parameter m for MMSE, ZF, and MRT. All results correspond to Scenario 1. When we increase the number of antennas, the spectral efficiency is increased significantly. For example, at $M = 10$, the spectral efficiency with MMSE is increased around 1.3 bits/s/Hz comparing with $M = 5$.

All precoders are compared in Figure 4.12. MMSE performs the best spectral efficiency with different parameters m at 0 dB SNR. For comparison between ZF and MRT, at the small number of antennas, the spectral efficiencies with ZF and MRT are very close with all parameters m. When we increase M, ZF is the better spectral efficiency than MRT with all parameters m.

4.2.2 Scenario 4

With this scenario, we increase the number of users in a massive MU-MIMO downlink system over Nakagami-m fading channel. We set the number of antennas $M = 20$. Furthermore, we choose SNR at 0 dB. We increase the number of users from 2 to 20. All results are shown in figures below.
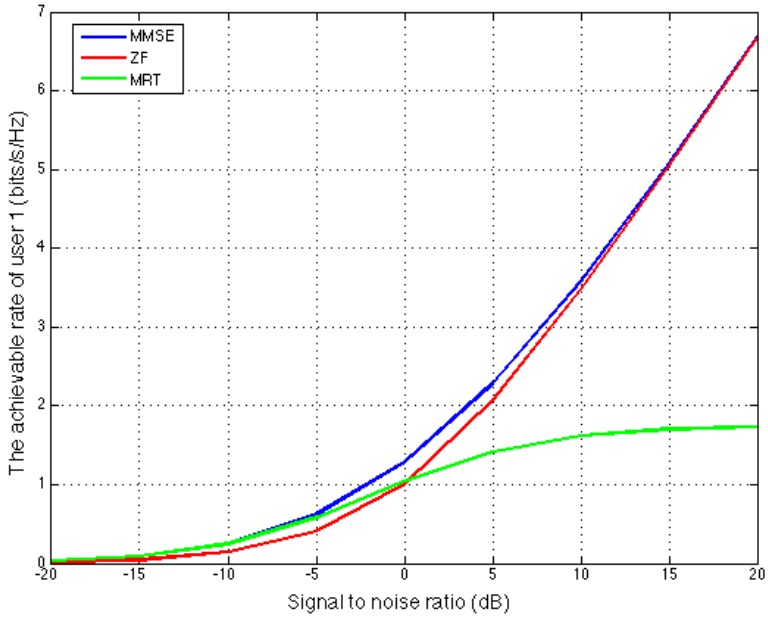
Figure 4.14 shows the spectral efficiency of massive MU-MIMO with MMSE over Nakagami-m fading. The spectral efficiency drops when many users access the system. At the beginning, the spectral efficiencies with MMSE increase by increasing the number of users. Until $K = 14$, the sum-rates increase very slowly.

Further, the sum-rates reduce with $K > 16$. With MMSE, the optimal number of users is around 16.

The result of spectral efficiency with ZF is shown in Figure 4.15. The sum-rate increases rapidly when the number of users increases. Until $K > 12$, the sum-rate with ZF is decreased quickly by increasing the number of users. the optimal number of users is around 25 for a massive MU-MIMO downlink system over Nakagami-m fading channel with $M = 20$.

Figure 4.16 shows that the spectral efficiency with MRT is increased slowly by increasing the number of users. The sum-rate still increases although the number of users is getting close the number of antennas.

All results in Scenario 4 are compared in Figure 4.17. This figure shows that the spectral efficiency with MMSE gives the highest sum-rate although the number of users K increase. ZF preforms the higher spectral efficiencies than MRT. However, the spectral efficiencies with ZF and MRT are very nearby with $K \to M$

Figure 4.1. The achievable rate of user 1 with different SNR for MMSE, ZF and MRT over Rayleigh fading channel. In this example, $M = 20$, and $K = 10$.
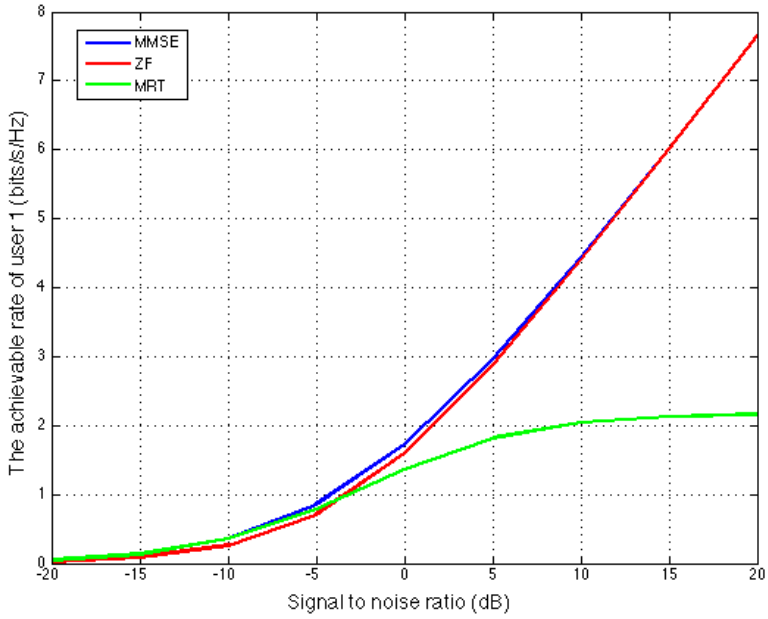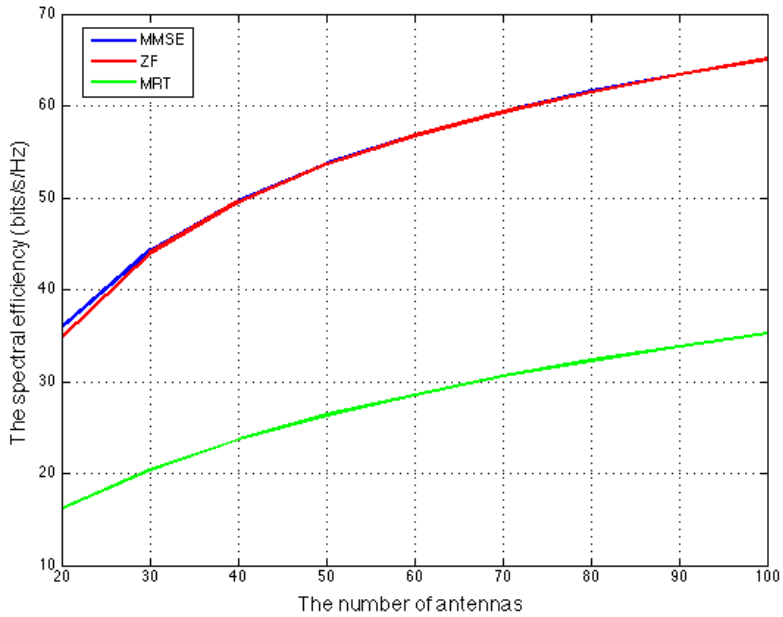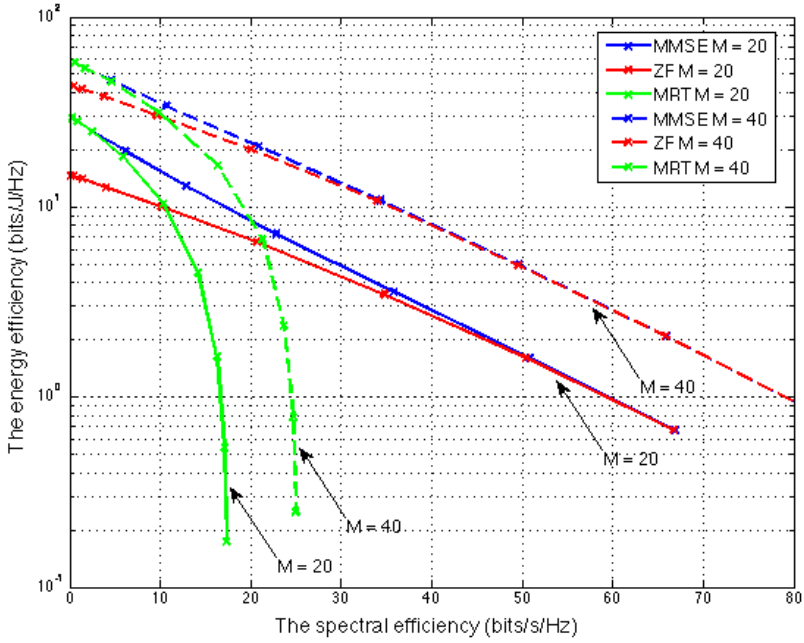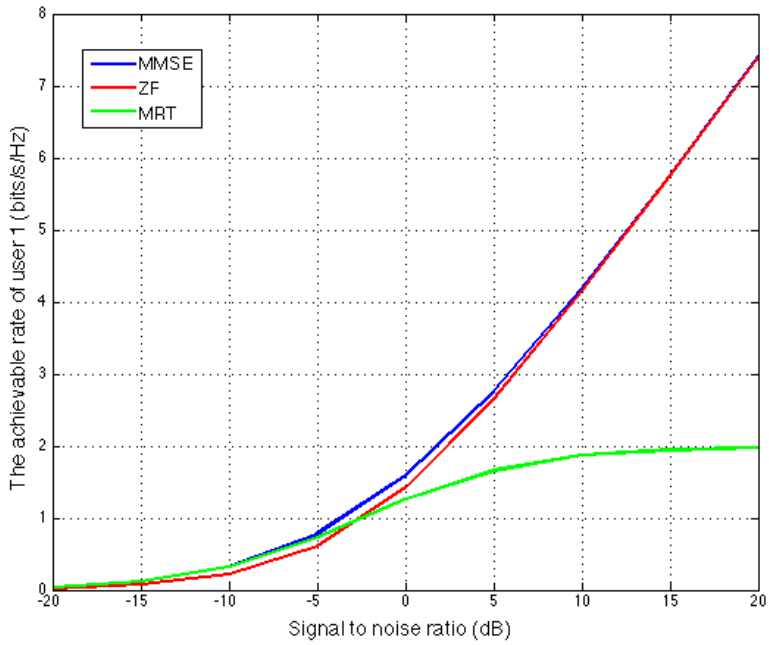
Figure 4.2. Same as Figure 4.1 but with $M = 40$.

Figure 4.3. The spectral efficiency versus the number of antennas over Rayleigh fading channel for MMSE, ZF, and MRT. In this example, $K = 10$ and SNR = 10 dB.

Figure 4.4. The energy efficiency VS spectral efficiency over Rayleigh fading channel with different number of antennas for MMSE, ZF, and MRT.

Figure 4.5. The achievable rate of user 1 with different SNR for MMSE, ZF and MRT over Rayleigh fading channel. In this example, $M = 40$, and $K = 15$.
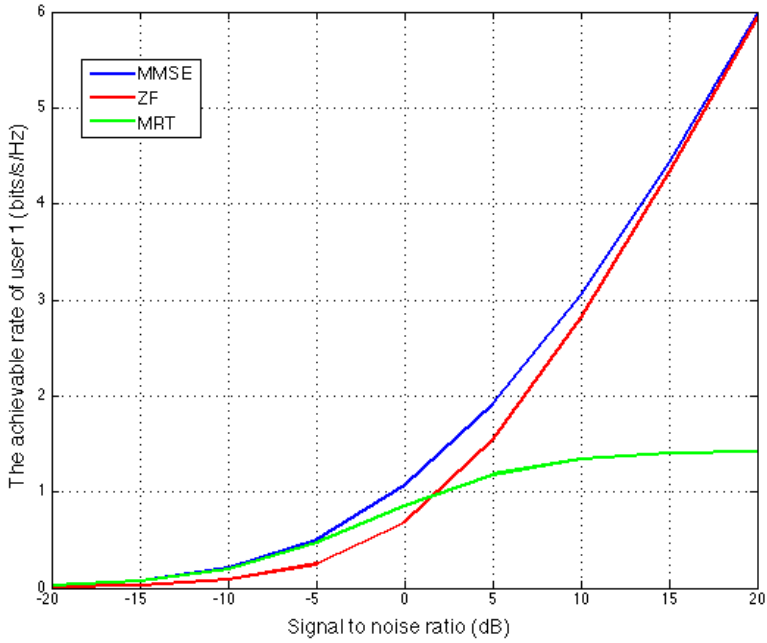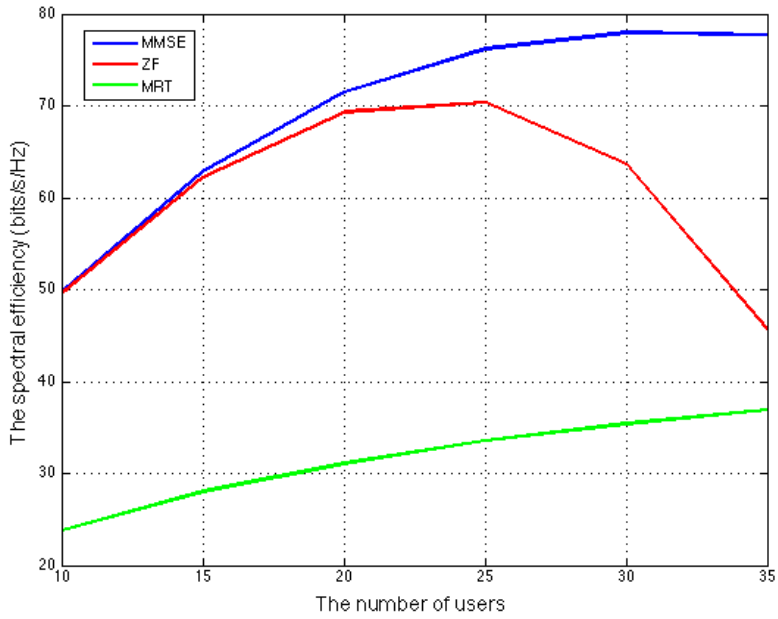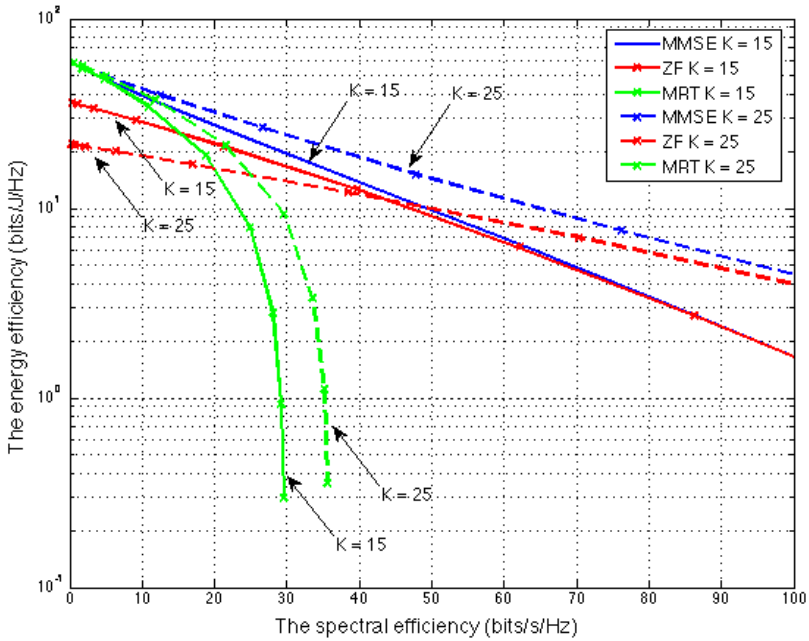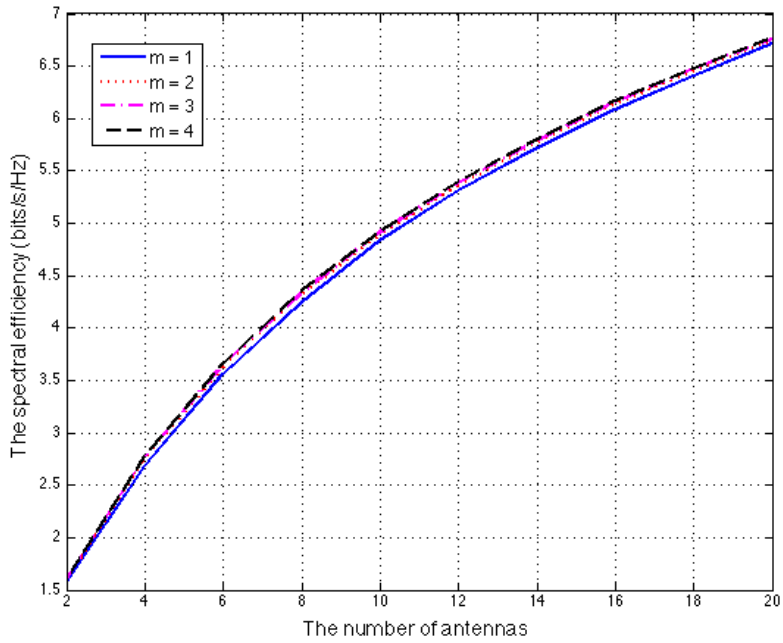
Figure 4.6. Same as Figure 4.5 but with $K = 25$.

Figure 4.7. The spectral efficiency versus number of users over Rayleigh fading channel for MMSE, ZF, and MRT. In this example, $M = 40$ and SNR $= 10$ dB

Figure 4.8. The energy efficiency VS spectral efficiency over Rayleigh fading channel with different number of users for MMSE, ZF, and MRT.

Figure 4.9. The spectral efficiency over Nakagami-m fading channel with different number of antennas for MMSE. In this example, $K = 2$ and SNR $= 0$ dB.
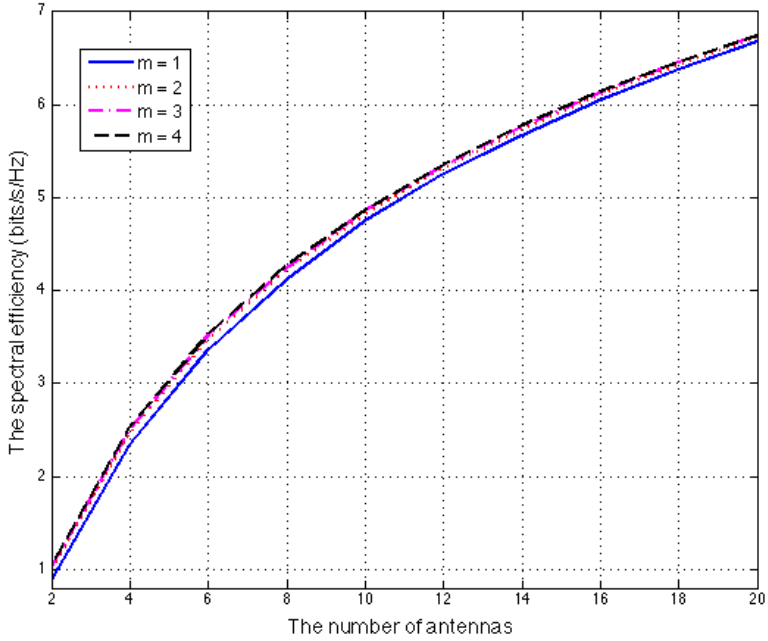
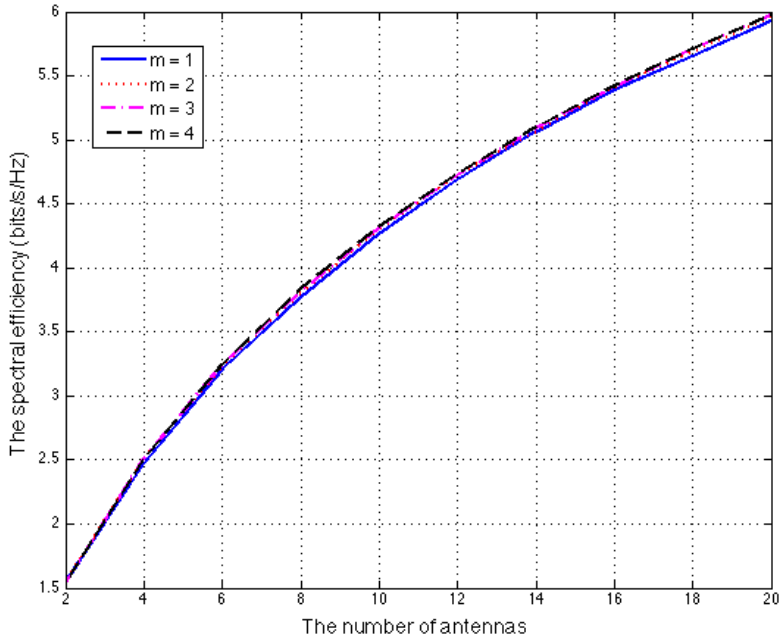**Figure 4.10.** Same as Figure 4.9 but for ZF.

Figure 4.11. Same as Figure 4.9 but for MRT.

Figure 4.12. The spectral efficiency versus the number of antennas over Nakagami-m Fading channel for MMSE, ZF, and MRT. In this example, $K = 2$ and SNR $= 0$ dB. At low SNR, MRT is better than ZF corresponding to Figure 4.1.
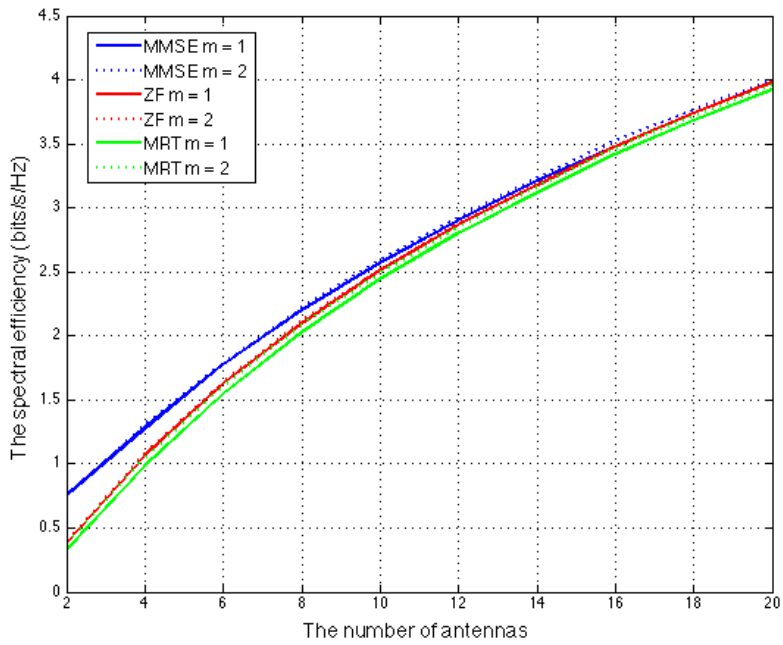
Figure 4.13. Same as Figure 4.12 but SNR = -5 dB.
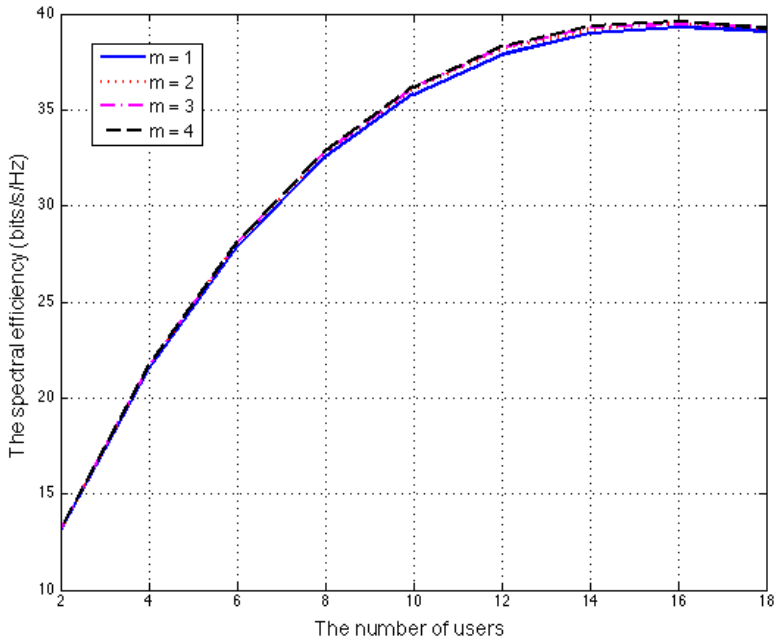
Figure 4.14. The spectral efficiency over Nakagami-m fading channel with different number of users for MMSE. In this example, $M = 20$ and SNR $= 0$ dB.
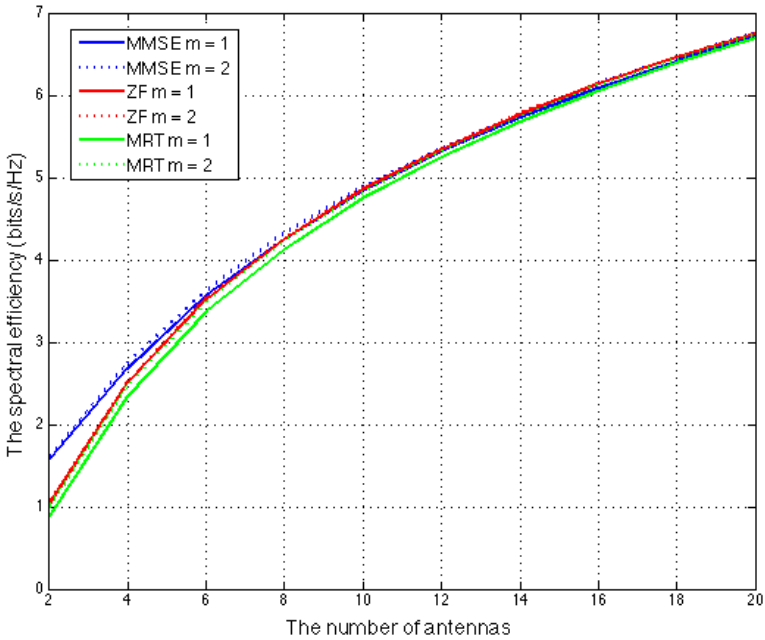
Figure 4.15. Same as Figure 4.14 but with ZF.

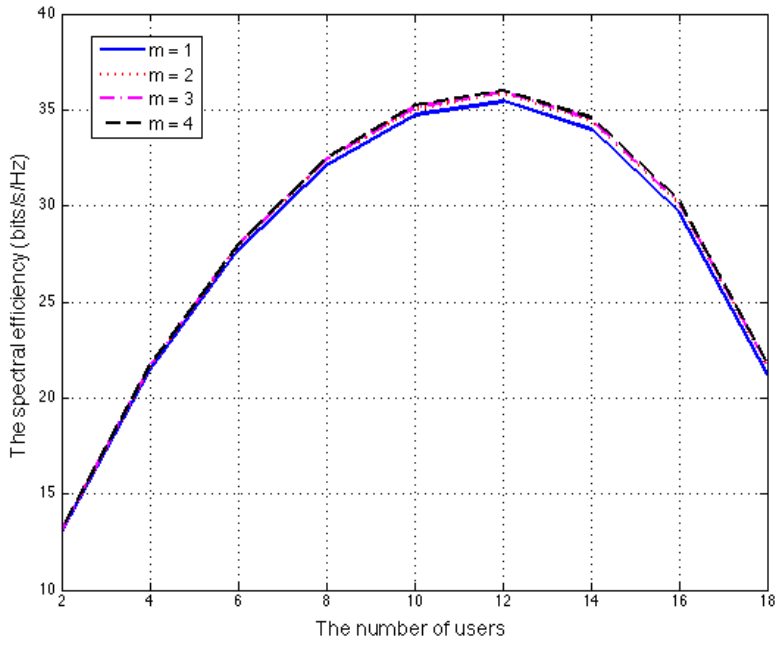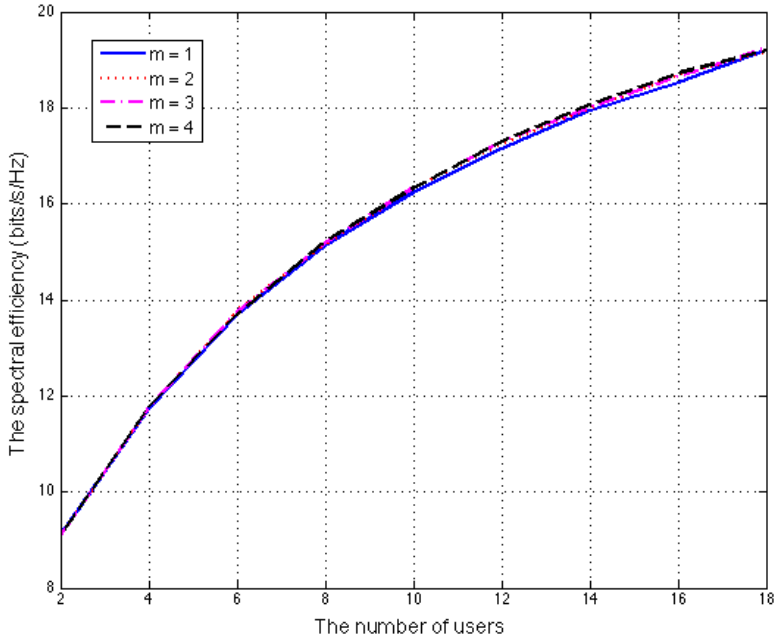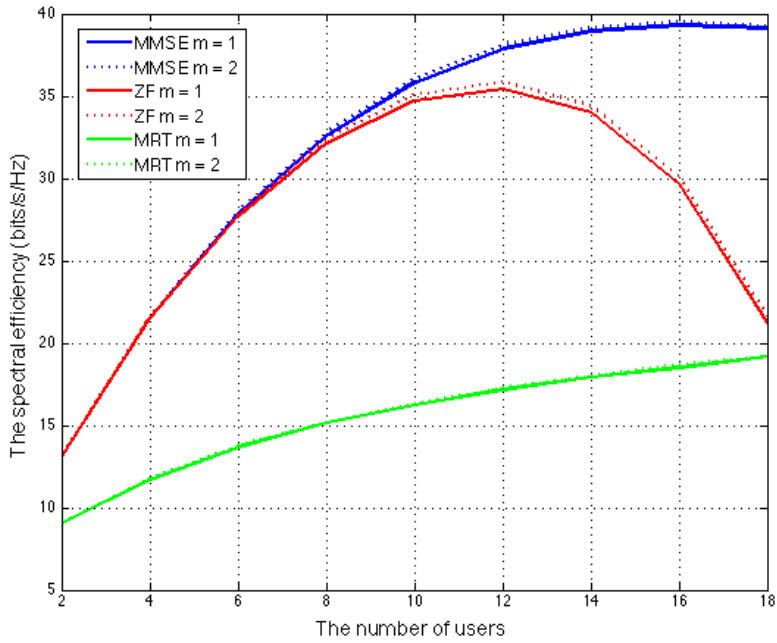**Figure 4.16.** Same as Figure 4.14 but with MRT

Figure 4.17. The spectral efficiency over Nakagami-m Fading channel versus the number of users for MMSE, ZF, and MRT. In this example, $M = 20$ and SNR $= 0$ dB.

4.3   Pratical Massive MU-MIMO System

The simulation results show that the massive MU-MIMO system gives the high performance in terms of the spectral efficiency and the energy efficiency. Therefore, we can apply this system to a practical system. We consider the effect of massive MU-MIMO system in the practical system, which includes orthogonal frequency division multiplex (OFDM), amplifiers, reliability, and phase noise.

4.3.1   Orthogonal Frequency Division Multiplexing

In the current wireless generation such as LTE, a MU-MIMO system uses Orthogonal Frequency Division Multiplexing (OFDM) to modulate the digital data to multiple sub-carrier frequencies. The advantages of OFDM on the MU-MIMO system are to change the multipath environments from frequency selective to flat fading, and to eliminate intersymbol interference (ISI).

From the simulation, we do not consider the massive MU-MIMO system over frequency selective fading channel. We assume that the multipath environment is flat. Our system model captures well what happen in the OFDM system with flat fading.

4.3.2   Amplifiers

In practice, the transmission power is very costly. The power consumption at the base station is constrained. Our model does not take dissipation in the power amplifier into account, per-antenna constraints into account, coupling between antennas and feeding chains into account [25].

4.3.3   Reliability

In the wireless communication, the robustness of the system is very important. One of many factors that affect the robustness of the system is the channel capacity or the achievable rate of the system. The high achievable rate gives the low robustness. See Figure 4.18. To eliminate this problem, coding is used for increasing data rate. For example, in LTE-Advanced, the base station provides the voice data for each user with the optimal rate. However, the voice communication is affected by bad channels between the base station and the user.

Some of the massive MIMO capacity increase can be used to send more error correcting bits, hence trading capacity for increased robustness.

4.3.4   Phase Noise

From scenarios 1 and 3, we know that increasing the number of antennas improves the performance of massive MU-MIMO system with perfect CSI in terms of the spectral efficiency, and the energy efficiency. However, we do not consider the error from the electronic circuits in our models.

According to [9], a phase noise is introduced in a frequency selective MU-MIMO system. At the transmitter, a baseband signal is up-converted to a passband signal
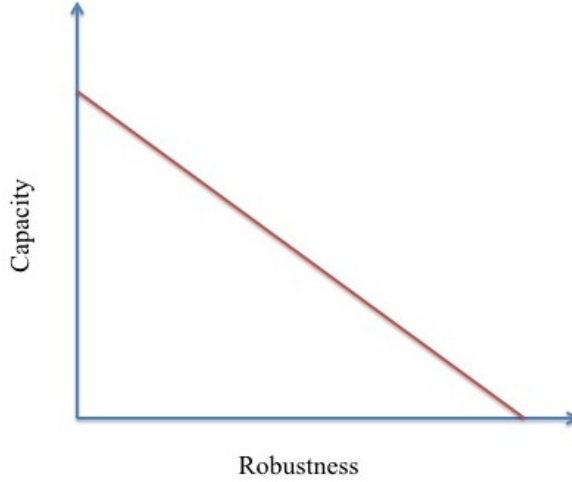
Figure 4.18. The capacity versus the robustness

by multiplication with a carrier frequency, which is generated by the oscillator. The phase of the carrier signal varies in time. Therefore, the phase of the passband signal has an error. At the receiver, the oscillator produces the phase error in the down-conversion process. In addition to phase error at the oscillator, the phase error occurs at each antenna element. All phase errors are called the phase noise. From the frequency selective MU-MIMO system, the spectral efficiency is lost by the phase noise. This is the conclusion of the paper [9]. Therefore, the massive MU-MIMO system should consider the phase noise in the system to obtain the exact performance.

Chapter 5

Conclusion

A massive MIMO system introduces the opportunity of increasing the spectral efficiency (in terms of bits/s/Hz) and improving the energy efficiency (in terms of bits/J) simultaneously. This system is able to use a simple processing such as MMSE, ZF, and MRT at the base station and using channel estimation from the uplink. Generally, ZF gives better performances at high transmission power while MRT gives better performance at the low transmission power. However, MMSE gives the best performance at low and high transmission power. Besides massive MU-MIMO can use a simple processing, the propagation environment does not affect much on the system performance. With a practical channel model without interference such as the Nakagami-m fading channel, the massive MU-MIMO system with the linear precoding improves the performance with different parameters m when the number of antennas was increased. Therefore, a massive MU-MIMO system is a key in next wireless system. It presents advantages in terms of the achievable rate, the spectral efficiency, and the energy efficiency.

Appendix A

Derivations of MMSE Precoding of MU-MIMO Downlink System

The derivations follow [20]. From (2.7), we have

$$\epsilon = \mathbb{E}\left[\|\beta\boldsymbol{y} - \boldsymbol{x}\|^2\right] \tag{A.1}$$

where $\boldsymbol{y}$ is a received signal vector, $\boldsymbol{x}$ is a transmitted signal vector, $\boldsymbol{A}$ is a precoding matrix and β is a scalar of Wiener filter. We find the precoding matrix $\boldsymbol{A}$ and β to minimize the MSE under the average power constrain P_{tr}; i.e.,

$$\left[\hat{\boldsymbol{A}}, \hat{\beta}\right] = \arg\min_{\boldsymbol{A},\beta} \epsilon$$
$$\text{s.t.}\,\mathbb{E}\left[\|\boldsymbol{s}\|^2\right] = P_{tr} \tag{A.2}$$

To solve the optimazation problem (A.2), we use the Lagrangian method. We define the Lagrangian function as follows:

$$\mathcal{L}\left(\boldsymbol{A}, \beta, \lambda\right) = \epsilon - \lambda\left(\text{tr}\left(\boldsymbol{A}^H\boldsymbol{A}\right) - P_{tr}\right) \tag{A.3}$$

where $\lambda \in \mathbb{R}$ is the Lagrangian factor Firstly, we take a derivative with respect to $\boldsymbol{A}$. We obtain

$$\frac{\partial\mathcal{L}\left(\boldsymbol{A}, \beta, \lambda\right)}{\partial\boldsymbol{A}} = 2\beta^2\boldsymbol{H}^*\boldsymbol{H}^T\boldsymbol{A} - 2\lambda\boldsymbol{A} - 2\beta\boldsymbol{H}^* = 0 \tag{A.4}$$

$$\tag{A.5}$$

Therefore,

$$\boldsymbol{A}\left(\mu\right) = \frac{1}{\beta}\boldsymbol{H}^*\left(\boldsymbol{H}^T\boldsymbol{H}^* + \mu\boldsymbol{I}_K\right)^{-1} \tag{A.6}$$

where we replace $-\frac{\lambda}{\beta^2}$ by $\mu \in \mathbb{R}$. Owing to the power constrain in (A.2), β can be represented as a function of μ. More precisely,

$$\beta(\mu) = \sqrt{\frac{\text{tr}\left(\boldsymbol{H}^T \boldsymbol{H}^* \left(\boldsymbol{H}^T \boldsymbol{H}^* + \mu \boldsymbol{I}_K\right)^{-2}\right)}{P_{tr}}} \tag{A.7}$$

Therefore, the constrained optimization problem with respect to $\boldsymbol{A}$ and β can be reduced to an unconstrained optimization problem with respect to μ. More precisely,

$$\hat{\mu} = \arg\min_{\mu} \epsilon\left(\boldsymbol{A}(\mu), \beta(\mu)\right) \tag{A.8}$$

We take a derivative with respect to μ equal to zero and we can obtain

$$\begin{aligned} \hat{\mu} &= \frac{\text{tr}(\boldsymbol{I}_K)}{P_{tr}} \\ &= \frac{K}{P_{tr}} \end{aligned} \tag{A.9}$$

Substituting (A.9) into (A.7) and (A.8), the optimal MMSE precoding $\boldsymbol{A}$ is given by

$$\hat{\boldsymbol{A}} = \frac{1}{\hat{\beta}} \boldsymbol{H}^* \left(\boldsymbol{H}^T \boldsymbol{H}^* + \frac{K}{P_{tr}} \boldsymbol{I}_K\right)^{-1} \tag{A.10}$$

where $\hat{\beta} = \sqrt{\frac{\text{tr}\left(\boldsymbol{H}^T \boldsymbol{H}^* \left(\boldsymbol{H}^T \boldsymbol{H}^* + \frac{K}{P_{tr}} P_{tr} \boldsymbol{I}_K\right)^{-2}\right)}{P_{tr}}}$

Bibliography

[1] F. Rusek, D. Persson, B. K. Lau, E. Larsson, T. Marzetta, O. Edfors, and F. Tufvesson, "Scaling up MIMO: Opportunities and challenges with very large arrays," *Signal Processing Magazine, IEEE*, vol. 30, no. 1, pp. 40–60, 2013.

[2] H. Q. Ngo, E. G. Larsson, and T. L. Marzetta, "Energy and spectral efficiency of very large multiuser MIMO systems," *Communications, IEEE Transactions on*, vol. 61, no. 4, pp. 1436–1449, 2013.

[3] P. Viswanath and D. Tse, "Sum capacity of the vector Gaussian broadcast channel and uplink-downlink duality," *IEEE Transactions on, Information Theory*, vol. 49, no. 8, pp. 1912–1921, 2003.

[4] H. Weingarten, Y. Steinberg, and S. Shamai, "The capacity region of the Gaussian multiple-input multiple-output broadcast channel," *Information Theory, IEEE Transactions on*, vol. 52, no. 9, pp. 3936–3964, 2006.

[5] A. Fehske, G. Fettweis, J. Malmodin, and G. Biczok, "The global footprint of mobile communications: The ecological and economic perspective," *Communications Magazine, IEEE*, vol. 49, no. 8, pp. 55–62, 2011.

[6] J. Hoydis, S. ten Brink, and M. Debbah, "Massive mimo in the UL/DL of cellular networks: How many antennas do we need?" *Selected Areas in Communications, IEEE Journal on*, vol. 31, no. 2, pp. 160–171, 2013.

[7] N. Krishnan, R. Yates, and N. Mandayam, "Cellular systems with many antennas: Large system analysis under pilot contamination," in *Communication, Control, and Computing (Allerton), 2012 50th Annual Allerton Conference on*, 2012, pp. 1220–1224.

[8] A. Pitarokoilis, S. Mohammed, and E. Larsson, "On the optimality of single-carrier transmission in large-scale antenna systems," *Wireless Communications Letters, IEEE*, vol. 1, no. 4, pp. 276–279, 2012.

[9] ——, "Effect of oscillator phase noise on uplink performance of large MU-MIMO systems," in *Communication, Control, and Computing (Allerton), 2012 50th Annual Allerton Conference on*, 2012, pp. 1190–1197.

[10] B. Gopalakrishnan and N. Jindal, "An analysis of pilot contamination on multi-user MIMO cellular systems with many antennas," in *Signal Processing Advances in Wireless Communications (SPAWC), 2011 IEEE 12th International Workshop on*, 2011, pp. 381–385.

[11] H. Q. Ngo, T. Duong, and E. Larsson, "Uplink performance analysis of multicell MU-MIMO with zero-forcing receivers and perfect CSI," in *Communication Technologies Workshop (Swe-CTW), 2011 IEEE Swedish*, 2011, pp. 40–45.

[12] H. Ngo, E. Larsson, and T. Marzetta, "The multicell multiuser MIMO uplink with very large antenna arrays and a finite-dimensional channel," pp. 1–12, 2013.

[13] X. Artiga, B. Devillers, and J. Perruisseau-Carrier, "Mutual coupling effects in multi-user massive MIMO base stations," in *Antennas and Propagation Society International Symposium (APSURSI), 2012 IEEE*, 2012, pp. 1–2.

[14] H. Q. Ngo and E. Larsson, "EVD-based channel estimation in multicell multiuser MIMO systems with very large antenna arrays," in *Acoustics, Speech and Signal Processing (ICASSP), 2012 IEEE International Conference on*, 2012, pp. 3249–3252.

[15] K. Vardhan, S. Mohammed, A. Chockalingam, and B. Rajan, "A low-complexity detector for large mimo systems and multicarrier CDMA systems," *Selected Areas in Communications, IEEE Journal on*, vol. 26, no. 3, pp. 473–485, 2008.

[16] T. Datta, N. Ashok Kumar, A. Chockalingam, and S. Rajan, "A novel monte carlo sampling based receiver for large-scale uplink multiuser MIMO systems," pp. 1–1, 2013.

[17] B. Bandemer, M. Haardt, and S. Visuri, "Linear MMSE multi-user MIMO downlink precoding for users with multiple antennas," in *Personal, Indoor and Mobile Radio Communications, 2006 IEEE 17th International Symposium on*, 2006, pp. 1–5.

[18] E. G. Larsson, F. Tufvesson, O. Edfors, and T. L. Marzetta, "Massive MIMO for Next Generation Wireless Systems," *IEEE Communications Magazine*, Apr. 2013.

[19] H. Q. Ngo, *Performance bounds for very large multiuser MIMO Systems*. LiU-Tryck, 2012.

[20] M. Joham, K. Kusume, M. H. Gzara, W. Utschick, and J. Nossek, "Transmit wiener filter for the downlink of TDD DS-CDMA systems," in *Spread Spectrum Techniques and Applications, 2002 IEEE Seventh International Symposium on*, vol. 1, 2002, pp. 9–13 vol.1.

[21] L. Ahlin, *Principles of wireless communications*. Studentlitteratur AB, 2006.

[22] G. Fraidenraich, O. Leveque, and J. Cioffi, "On the MIMO channel capacity for the Nakagami-m channel," in *Global Telecommunications Conference, 2007. GLOBECOM '07. IEEE*, 2007, pp. 3612–3616.

[23] U. Madhow, *Fundamentals of digital communication.* Cambridge University Press, 2008.

[24] T. Marzetta and B. Hochwald, "Fast transfer of channel state information in wireless systems," *Signal Processing, IEEE Transactions on*, vol. 54, no. 4, pp. 1268–1278, 2006.

[25] D. Persson, T. Eriksson, and E. Larsson, "Amplifier-aware multiple-input multiple-output power allocation," pp. 1–4, 2013.